GEOPHYSICAL RESEARCH LETTERS, VOL. 37, L11304, doi:10.1029/2010GL043220, 2010

Crustal-scale pure shear foreland deformation of western Argentina

Andrew J. Meigs[1] and John Nabelek[2]

Received 15 March 2010; revised 7 May 2010; accepted 12 May 2010; published 11 June 2010.

[1] New analyses of teleseismic body waves from moderate earthquakes in western Argentina demonstrate that active shortening of the Andean foreland occurs on reverse faults extending to 40–50 km depth. Existing crustal-scale models of foreland deformation invoke thin-skinned fault geometries, which root into an east-dipping mid-crustal décollement. Whereas thin-skinned thrust sheets dominate shallow-crustal structure, seismological and geological data illustrate that planar reverse faults and pure-shear deformation involving more than 75% of the crust characterizes this thick-skinned structural province. **Citation:** Meigs, A. J., and J. Nabelek (2010), Crustal-scale pure shear foreland deformation of western Argentina, *Geophys. Res. Lett.*, *37*, L11304, doi:10.1029/2010GL043220.

1. Introduction

[2] Deformation in foreland fold-and-thrust belts commonly shifts from shallow, thin-skinned faults to deep, thick-skinned structures in time and space [*Wiltschko and Dorr*, 1983]. The observation that thin-skin (shallow) thrust faults root into a dipping basal décollement implies that simple shear characterizes the strain at the whole-orogen scale. A simple shear strain-state is also commonly inferred for Laramide-style structural provinces; thick-skinned reverse-faulted regions found along the foreland periphery of thrust belts [*Erslev*, 1993; *Oldow et al.*, 1989]. Few direct data, however, constrain fault geometries at the crustal-scale. Earthquakes in active Laramide-style provinces provide constraint on the style of deep deformation.

[3] In this paper, we present a new model for active thick-skinned deformation of the Sierras Pampeanas structural province in western Argentina, the type-example of active Laramide-style deformation [*Jordan and Allmendinger*, 1986]. The model reconciles a new analysis of teleseismic body waves from the Ms = 7.4, 11 June, 1944 San Juan earthquake [*Castellanos*, 1945], recent earthquakes, and regional geologic relationships. Source parameters of the 1944 San Juan and other earthquakes indicate that planar active faults extend to 40–50 km, which favors a whole-crust pure shear model for Laramide-style orogenesis.

2. Seismicity and Active Tectonics of Northwest Argentina

[4] The Sierras Pampeanas lie above the flat slab segment of the Nazca Plate [*Cahill and Isacks*, 1992]. Structure to the west comprises the east-vergent thin-skinned central Precordillera (Figure 1) [*Ramos et al.*, 2002]. A structural province of mixed thin- and thick-skinned faults, the eastern Precordillera, separates the two provinces [*Fielding and Jordan*, 1988; *Zapata and Allmendinger*, 1996]. Existing models offer a variety of interpretations of the crustal-scale architecture of the active faults. In most models mapped surface faults decrease dip with depth [e.g., *Jordan and Allmendinger*, 1986; *Zapata and Allmendinger*, 1996], which root into a speculative low-angle décollement at 15 to 30 km depths in another group of models [*Alvarado and Beck*, 2006; *Ramos et al.*, 2002; *Siame et al.*, 2002].

[5] Seismicity, dominated by reverse faulting mechanisms, occurs to depths greater than 40 km under the eastern Precordillera and Sierras Pampeanas (Figure 1) [*Alvarado et al.*, 2005; *Smalley et al.*, 1993]. Surface deformation associated with moderate earthquakes in 1977 and 1944 consisted of fold growth and limited slip on secondary faults [*Kadinsky-Cade et al.*, 1985; *Meigs et al.*, 2006]. Whereas the 1977 Caucete earthquake sequence is consistent with regional seismicity [*Kadinsky-Cade et al.*, 1985], the shallow 11 km depth of the 1944 event [*Alvarado and Beck*, 2006] seems atypical.

3. Source Parameters of the 1944 San Juan Earthquake

[6] We modeled long-period teleseismic body waveforms to independently determine the depth, moment, and focal mechanism of the 1944 event (Table S1 in Text S1 in the auxiliary material) [*Nabelek*, 1984].[3]

[7] Four stations at epicentral distances between 30° and 90° (required for the modeling) provided excellent teleseismic P and SH records (Table S2 in Text S1 and Figure 2). Theoretical seismograms were computed by assuming a point source using *Shearer et al.*'s [2002] velocity model (Table S3 in Text S1) and attenuation parameter t* = 0.70 s for P waves and t* = 4.5 s for SH waves. Synthetic waveforms were fit in a least-squares sense to the observed displacement waveforms to determine the best-fitting double-couple source (Figure 2). Converting seismograms to displacement is crucial for obtaining stable results.

[8] We performed a number of inversions to investigate the stability of the results. A 30-s-long source time function

[1]Department of Geosciences, Oregon State University, Corvallis, Oregon, USA.
[2]College of Oceanic and Atmospheric Sciences, Oregon State University, Corvallis, Oregon, USA.

0094-8276/10/2010GL043220

[3]Auxiliary materials are available in the HTML. doi:10.1029/2010GL043220.

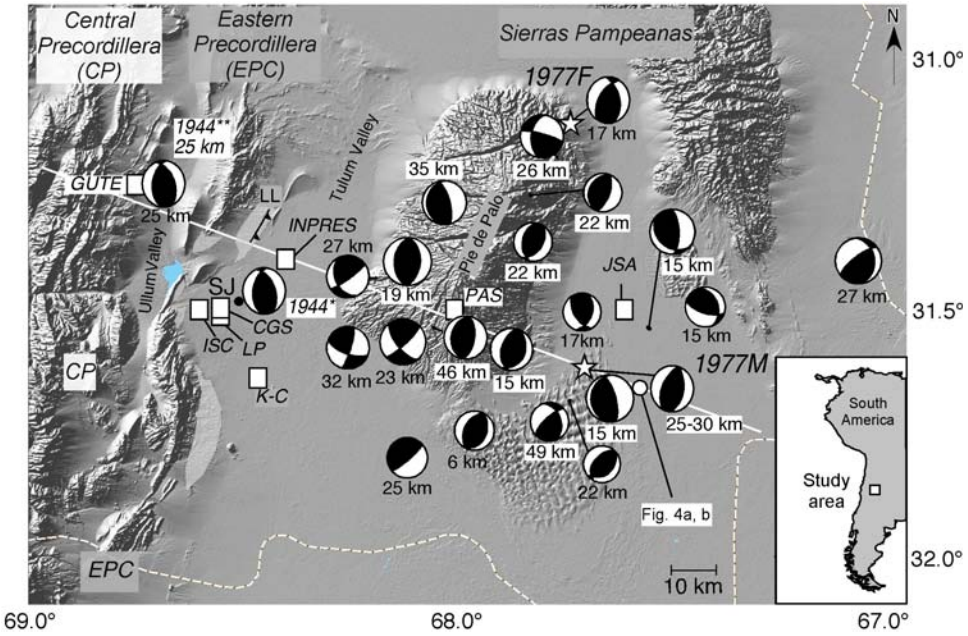

Figure 1. Map of the Andean foreland in northwest Argentina in the region of San Juan (SJ). Cross-hatched polygons demark domains of active folding and fold-related faulting, including the La Laja fault (LL). The centroidal focal mechanisms are from the Harvard CMT catalogue, *Kadinsky-Cade* [1985], *Alvarado et al.* [2005] and this study (asterisks). Locations of Caucete foreshock (1977F) and main shock (1977M) are indicated by stars. 1944 earthquake locations (white boxes): GUTE, Gutenberg; ISC, International Seismological Centre; CGS, Coastal and Geodetic Survey; LP, La Plata Bulletin; K-C, *Kadinsky-Cade* [1985]; INPRES, Instituto Nacional de Prevención Sísmica; PAS, Pasadena Bulletin; JSA, Jesuit Seismological Association Bulletin (Table S2 in Text S1). Solid white line marks cross-section in Figures 4a and 4b. Base map made from a USGS DEM. White dotted line denotes provincial borders.

parameterization enabled unbiased source depth estimates in the presence of a potentially complex source time history. The 4 SH waves, which, except for CHR, are close to nodal, provide strong constraint on the source mechanism and depth (particularly PAS (Figure 2a)). The centroid mechanism indicates a Mw 6.9 dip-slip event with a small strike-slip component; one nodal plane (P1) strikes to 364° 84 and dips 47° E and the other nodal plane (P2) strikes to 208° and dips 52° W (Table S1 in Text S1). The source time function reveals a ~6 s-long simple impulsive event. A well-resolved centroid depth of 25 km is consistent with both the P and SH waveforms (Figures 2a and 3). A 25 km depth compares well with other moderate earthquakes and microseismicity regionally (Figure 1) [*Alvarado et al.*, 2007; *Smalley et al.*, 1993].

[9] *Alvarado and Beck* [2006] argue that the 1944 event had an 11 km depth and northeast- and northwest-striking nodal planes on the basis of P wave velocity seismograms. In order to compare approaches, we inverted the original P velocity seismograms as well. Depths between 5 and 12.5 km are essentially indistinguishable from a 25 km depth based on inversion of the velocity records (Figure 3). To match the waveforms, the solutions in the 5 to 12.5 km depth range require a complicated source time function. P-only inversions exhibit 90° rotation in fault strike as the centroid depth decreases from 25 to 5 km (Figure 3). These ambiguities arise because of the difficulties associated with distinguishing depth phases (pP, sP) from potential source time function complexity in velocity-based inversions. Use of displacement seismograms and the SH waves greatly stabilizes the inferred depth and the focal mechanism. The SH wave at PAS shows the best visual evidence that the event is not shallow (Figure 2).

4. Implications of Argentine Seismotectonics for Laramide-Style Deformation

[10] Candidate source faults of the 1944 earthquake include the east-dipping La Laja fault, because it slipped in the 1944 event [*Groeber*, 1944; *Harrington*, 1944], the east-dipping range-front thrust fault system bounding the western flank of the Eastern Precordillera [*Siame et al.*, 2002], and a northwest-dipping fault identified from microseismicity (Figures 1 and 4a) [*Smalley et al.*, 1993]. Neither the La Laja fault nor the range front fault, crustal faults that root into a shallow décollement (Figure 4a), likely represent the direct up-dip continuation of the seismogenic fault. The La Laja fault is a secondary flexural-slip fault [*Costa et al.*, 1999; *Meigs et al.*, 2006] and its strike differs by ~45° from the earthquake nodal plane strikes. Except for local flexural slip faulting with minor vertical offset, the range front thrust system does not cut surficial deposits [*Meigs et al.*, 2006; *Schiffman*, 2007]. Clearly, thin-skinned thrusts at the surface do not connect in a simple way to the earthquake source region.

[11] A blind reverse fault model for the 1944 event reconciles surface geology and seismologic observations. The impulsive 6 s source time function implies that the initial coseismic rupture did not reach the surface. If subsequent non-seismic process at shallow depths distributed the coseismic slip, a simple calculation using the seismic moment and fault dimensions shows that the expected slip

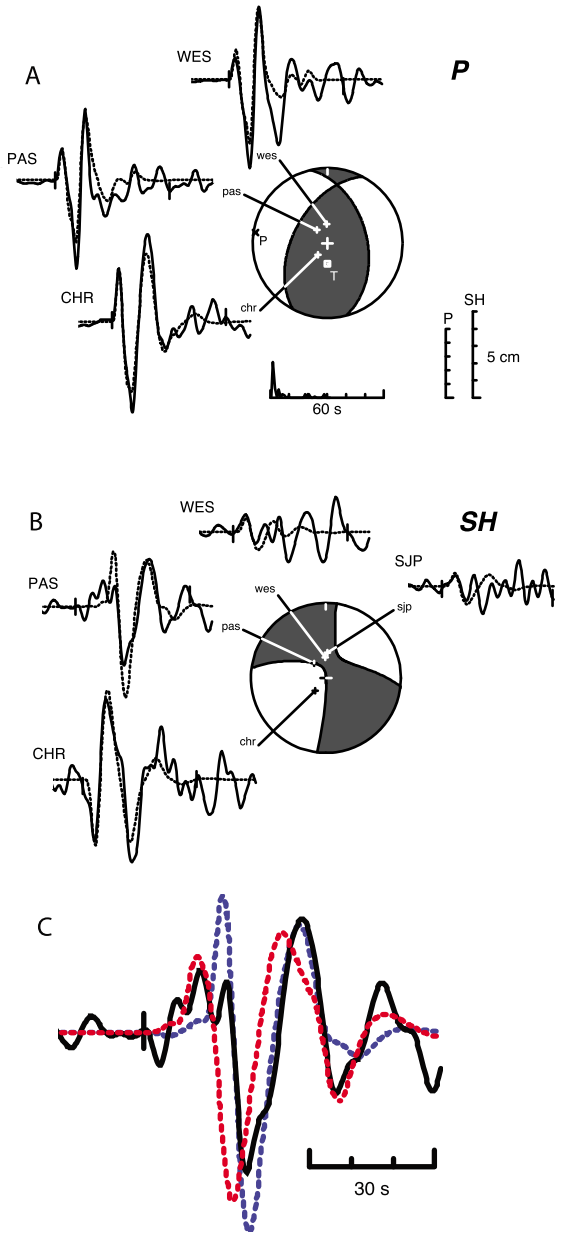

Figure 2. Modeled (a) P and (b) SH waves of the 1944 earthquake. Solid lines are the observed seismograms; the dashed lines are the best-fitting theoretical seismograms. Also shown are the P and SH radiation patterns and the estimated source time function. Stations include: Christchurch (CHR), Pasadena (PAS), San Juan, Puerto Rico (SJP), and Weston (WES). (c) SH displacement waveform recoded at PAS (black line). Black tick mark indicates the onset of the direct SH phase, which is nodal at this station. The later-arriving larger pulse is the reflected shSH phase. Blue line shows the fit for a source centroid at 25 km depth and red line for a source centroid at 11 km depth. The predicted arrival for the centroid at 11 km arrives about 5 s earlier than observed.

observed at the surface would be less than 20 cm. Active folding dominates the surface deformation and is expressed as southeast-facing monoclines on the eastern flank of the eastern Precordillera [*Meigs et al.*, 2006; *Vergés et al.*, 2007]. Secondary faults like the La Laja fault, which indicate active folding, occur within the limbs of the monoclines. If the location and geometry of active folds at the surface identifies the location of blind faults at depth, field data and microseismicity favor a simple blind, planar, and west-dipping fault that extends up- and down-dip from the 25 km centroid depth (Figure 4b) [*Meigs et al.*, 2006; *Smalley et al.*, 1993]. A west dip implies the epicenter lies to the west of San Juan (Figures 1 and Table S2 in Text S1) [*Gutenberg and Richter*, 1954]. If the epicenter is located near or to the east of San Juan (Figure 1) [*Alvarado and Beck*, 2006], the source fault dips east and extends below the western edge of the Sierras Pampeanas province (Figure 4b).

[12] Source parameters suggest that the Caucete earthquake sequence in 1977 and the 1944 event were similar (Figure 1). Pure thrust events characterize the 1977 foreshock and main shock, which originated beneath Pie de Palo [*Chinn and Isacks*, 1983; *Kadinsky-Cade*, 1985; *Triep*, 1984]. Nodal planes for the foreshock (Ms = 6.8, ~17 km depth) and the main shock (Ms = 7.3, ~25 km depth) dip at 35°–50° (Figure 1), although it is unclear whether the earthquake fault dips east or west [*Kadinsky-Cade et al.*, 1985; *Langer and Hartzell*, 1996]. Elastic dislocation modeling of the 1.2 meters of coseismic uplift indicates rupture from 17 to 30 km depth in the main shock [*Kadinsky-Cade et al.*, 1985]. Both the 1977 and the 1944 earthquakes occurred on planar blind thrust faults extending depths < 10 km to > 40 km at dips between 35° and 45° (Figure 4b).

[13] Owing to their presence along the periphery of fold-and-thrust belts [*Rodgers*, 1987], structural interpretations of Laramide-style basement faults often invoke a mid-crustal low-angle décollement at depth [*Erslev*, 1993]. An earthquake centroid represents a slip-weighted average from which coseismic slip extends up- and down-dip by roughly equal amounts. Fault plane rupture in the 25 km-deep M 6.9 1944 earthquake, for example, would occur ~10 km up- and

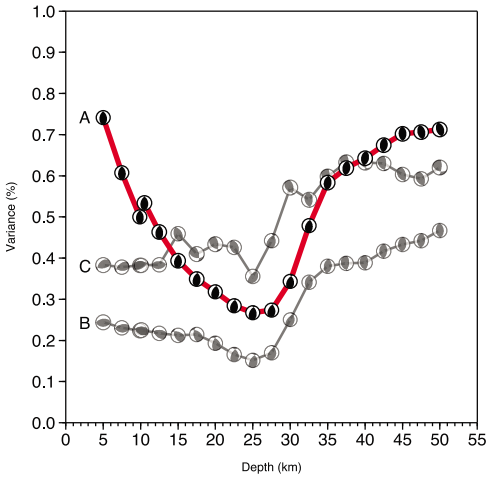

Figure 3. Misfit variance and source mechanism for three alternative inversions: inversion of P and SH low-frequency displacement seismograms (curve A); inversion of P wave low-frequency displacement seismograms (curve B); inversion original unfiltered velocity seismograms (curve C). Including both P and SH displacement waveforms stabilizes the mechanism and improves the depth resolution. See text for discussion.

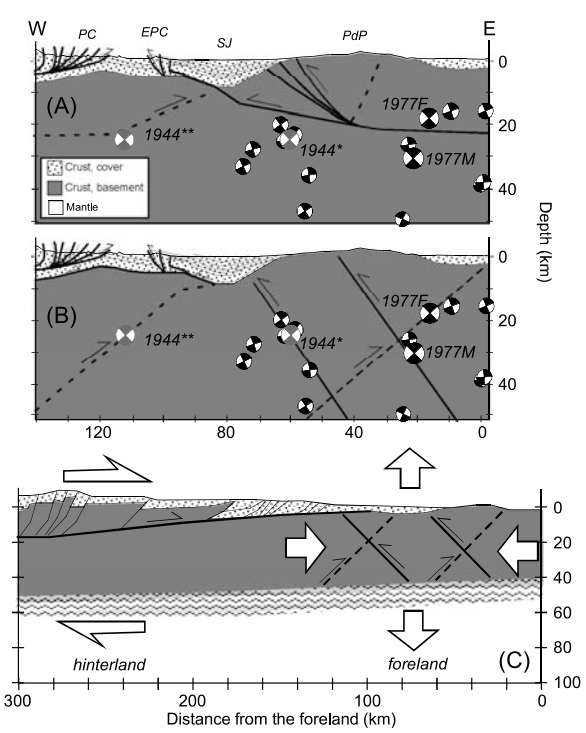

Figure 4. Crustal-scale models of western Argentina foreland structures. (a) Thin-skinned, mid-crustal décollement model [*Alvarado and Beck*, 2006; *Ramos et al.*, 2002; *Siame et al.*, 2002]. Caucete earthquake foreshock (1977F) and main shock (1977m) [*Kadinsky-Cade*, 1985] and eastern (asterisk) and western (double asterisk) alternatives for the 1944 San Juan earthquake (light grey symbols) marked. Surface geology modified from [*Cristallini and Ramos*, 2000; *Meigs et al.*, 2006; *Ramos et al.*, 2002]. EPC, Eastern Precordillera; PC, Precordillera; PdP, Pie de Palo; SJ, San Juan. (b) Planar fault interpretation [modified from *Kadinsky-Cade et al.*, 1985]. (c) Lithospheric scale cross-section contrasting fold-and-thrust belt simple shear strain with planar Laramide-style reverse faulting that implies pure shear strain and distributed lower crustal deformation (cross-hatch). Pure shear thickening of the seismogenic crust is likely accommodated in the lower crust by thickening or flow.

down-dip from the centroid depth [*Wells and Coppersmith*, 1994]. The centroid depths of moderate-magnitude earthquakes in our study region range from 6 to 49 km and are typified by nodal planes with 30° to 50° dips (Figure 1), which implies active faulting extends across the crust at moderate dips rather than localized on a shallowly-dipping décollement in the mid-crust (Figure 4b).

[14] A crustal-scale model where planar faults extend into the lower crust at moderate dip angles indicates that active Laramide-style deformation in western Argentina occurs via pure-shear crustal shortening (Figure 4c). Geophysical data reveal similar basement-involved fault geometries in Papua New Guinea, Iran, and the western U.S. [*Abers and McCaffrey*, 1988; *Berberian*, 1995; *Jackson*, 1980; *Smithson et al.*, 1978]. Neither listric geometries nor a regional décollement are consistent with moderately east and west dipping nodal planes on events as deep as 50 km (Figure 1). Given that the crust is ~55 km thick in the region of the 1944 and 1977 earthquakes [*Alvarado et al.*, 2007], more than 75% of the crust is deforming by seismic faulting on east- and west-dipping faults. A ~50 km-thick seismogenic crust implies a mafic composition, which is consistent with seismic velocity data [*Alvarado et al.*, 2005]. It should be stressed that crustal pure shear can occur in synchrony and independently of fold-and-thrust belt simple shear of the upper crustal (Figure 4c). Laramide-style shortening in the foreland occurs in response to overthickening of the crust in the thin-skinned thrust belt to the west [*Molnar and Lyon-Caen*, 1988], eliminating any need for structural linkage between Laramide and thin-skinned structures at depth beneath the orogen.

[15] **Acknowledgments.** We acknowledge support from NSF-EAR grants 0409443 and 0838538. We thank A. Bent, D. Smith, S. Hayek, B. Ferris, G. Atkinson, J. Cassidy, and R. Adams for help with the historical records. Discussion with E. Triep, P. Alvarado, and V. Ramos were particularly helpful.

References

Abers, G., and R. McCaffrey (1988), Active deformation in the New Guinea fold-and-thrust belt: Seismological evidence for strike-slip faulting and basement-involved thrusting, *J. Geophys. Res.*, *93*(B11), 13,332–13,354, doi:10.1029/JB093iB11p13332.

Alvarado, P., and S. Beck (2006), Source characterization of the San Juan (Argentina) crustal earthquakes of 15 January 1944 (M7.0) and 11 June 1952 (M6.8), *Earth Planet. Sci. Lett.*, *243*(3–4), 615–631, doi:10.1016/j.epsl.2006.01.015.

Alvarado, P., S. Beck, G. Zandt, M. Araujo, and E. Triep (2005), Crustal deformation in the south-central Andes backarc terranes as viewed from regional broad-band seismic waveform modelling, *Geophys. J. Int.*, *163*, 580–598, doi:10.1111/j.1365-246X.2005.02759.x.

Alvarado, P., S. Beck, and G. Zandt (2007), Crustal structure of the south-central Andes Cordillera and backarc region from regional waveform modelling, *Geophys. J. Int.*, *170*(2), 858–875, doi:10.1111/j.1365-246X.2007.03452.x.

Berberian, M. (1995), Master "blind" thrust faults hidden under the Zagros folds: Active basement tectonics and surface morphotectonics, *Tectonophysics*, *241*, 193–195, doi:10.1016/0040-1951(94)00185-C.

Cahill, T., and B. L. Isacks (1992), Seismicity and shape of the subducted Nazca Plate, *J. Geophys. Res.*, *97*(B12), 17,503–17,529, doi:10.1029/92JB00493.

Castellanos, A. (1945), Parte B. El terremoto de San Juan, in *Cuatro Lecciones Sobre Terremotos*, 242 pp., Asoc. Cult. de Conf. de Rosario, Rosario, Argentina.

Chinn, D. S., and B. L. Isacks (1983), Accurate source depths and focal mechanisms of shallow earthquakes in western South America and New Hebrides Island Arc, *Tectonics*, *2*(6), 529–563, doi:10.1029/TC002i006p00529.

Costa, C. H., T. Rockwell, J. Paredes, and C. Gardini (1999), Quaternary deformations and seismic hazard at the Andean orogenic front (31°–33°, Argentina), in *Fourth International Symposium on Andean Geodynamics, Extended Abstracts*, pp. 187–191, Inst. de Rech. pour le Dev., Paris.

Cristallini, E. O., and V. A. Ramos (2000), Thick-skinned and thin-skinned thrusting in the La Ramada fold and thrust belt: Crustal evolution of the High Andes of San Juan, Argentina (32°SL), *Tectonophysics*, *317*, 205–235, doi:10.1016/S0040-1951(99)00276-0.

Erslev, E. A. (1993), Thrusts, back-thrusts, and detachment of Rocky Mountain foreland arches, in *Laramide Basement Deformation in the Rocky Mountain Foreland of the Western United States*, edited by C. J. Schmidt et al., *Spec. Pap. Geol. Soc. Am.*, *280*, 339–358.

Fielding, E. J., and T. E. Jordan (1988), Active deformation at the boundary between the Precordillera and Sierras Pampeanas, Argentina, and comparison with ancient Rocky Mountain deformation, in *Interactions of the Rocky Mountain Foreland and the Cordilleran Thrust Belt*, edited by W. J. Perry and C. J. Schmidt, *Geol. Soc. Am. Mem.*, *171*, 143–163.

Groeber, P. (1944), Movimientos tectonicos contemporaneos y un nuevo tipo de dislocaciones, *Notas Mus. La Plata*, *9*(33), 363–375.

Gutenberg, B., and C. F. Richter (1954), *Seismicity of the Earth*, 2nd ed., 310 pp., Princeton Univ. Press, Princeton, N. J.

Harrington, H. J. (1944), *El Sismo de San Juan; del 15 de Enero de 1944*, 79 pp., Corp. para la Promocion del Intercambio, Buenos Aires.

Jackson, J. A. (1980), Reactivation of basement faults and crustal shortening in orogenic belts, *Nature*, *283*(5745), 343–346, doi:10.1038/283343a0.

Jordan, T. E., and R. W. Allmendinger (1986), The Sierras Pampeanas of Argentina: A modern analogue of Rocky Mountain foreland deformation, *Am. J. Sci.*, *286*(10), 737–764.

Kadinsky-Cade, K. (1985), Seismotectonics of the Chile margin and the 1977 Caucete earthquake of western Argentina, 253 pp., Ph.D. thesis, Cornell Univ., Ithaca, N. Y.

Kadinsky-Cade, K., R. Reilinger, and B. Isacks (1985), Surface deformation associated with the November 23, 1977, Caucete, Argentina, earthquake sequence, *J. Geophys. Res.*, *90*(B14), 12,691–12,700, doi:10.1029/JB090iB14p12691.

Langer, C. J., and S. Hartzell (1996), Rupture distribution of the 1977 western Argentina earthquake, *Phys. Earth Planet. Inter.*, *94*, 121–132, doi:10.1016/0031-9201(95)03080-8.

Meigs, A., W. C. Krugh, C. Schiffman, J. Vergés, and V. A. Ramos (2006), Refolding of thin-skinned thrust sheets by active thick-skinned thrust faults in the eastern Precordillera of San Juan Province, Argentina, *Asoc. Geol. Argent. Rev.*, *61*(4), 589–603.

Molnar, P., and H. Lyon-Caen (1988), Some simple physical aspects of the support, structure, and evolution of mountain belts, in *Processes in Continental Lithospheric Deformation*, edited by S. P. Clark Jr., B. C. Burchfiel, and J. Suppe, *Spec. Pap. Geol. Soc. Am.*, *218*, 179–207.

Nabelek, J. L. (1984), Determination of earthquake source parameters from inversion of body waves, Ph.D. thesis, 361 pp., Mass. Inst. of Technol., Cambridge.

Oldow, J. S., A. W. Bally, G. H. Lallemant, and W. P. Leeman (1989), Phanerozoic evolution of the North American Cordillera: United States and Canada, in *The Geology of North America*, vol. A, *The Geology of North America: An Overview*, edited by A. W. Bally and A. R. Palmer, pp. 139–232, Geol. Soc. of Am., Boulder, Colo.

Ramos, V. A., E. O. Cristallini, and D. J. Pérez (2002), The Pampean flat-slab of the central Andes, *J. South Am. Earth Sci.*, *15*(1), 59–78, doi:10.1016/S0895-9811(02)00006-8.

Rodgers, J. (1987), Chains of basement uplifts within cratons marginal to orogenic belts, *Am. J. Sci.*, *287*(7), 661–692.

Schiffman, C. (2007), Seismotectonics in the eastern Precordillera, San Juan, Argentina: Reconciling earthquakes and structural geology in the vicinity of the 1944 earthquake for a new model of crustal-scale deformation, M.S. thesis, 95 pp., Oregon State Univ., Corvallis.

Shearer, T., S. Beck, G. Zandt, and P. Alvarado (2002), Lithospheric structure of the Sierras Pampeanas, south central Andes, *Eos Trans. AGU*, *83*(47), Fall Meet. Suppl., Abstract S52A-1063.

Siame, L. L., O. Bellier, M. Sébrier, D. L. Bourlès, P. Leturmy, M. Perez, and M. Araujo (2002), Seismic hazard reappraisal from combined structural geology, geomorphology and cosmic ray exposure dating analyses: The eastern Precordillera thrust system (NW Argentina), *Geophys. J. Int.*, *150*(1), 241–260, doi:10.1046/j.1365-246X.2002.01701.x.

Smalley, R., Jr., J. Pujol, M. Regnier, J.-M. Chiu, J.-L. Chatelain, B. L. Isacks, M. Araujo, and N. Pueblas (1993), Basement seismicity beneath the Andean Precordillera thin-skinned thrust belt and implications for crustal and lithospheric behavior, *Tectonics*, *12*(1), 63–76, doi:10.1029/92TC01108.

Smithson, S. B., J. Brewer, S. Kaufman, J. Oliver, and C. Hurich (1978), Nature of the Wind River thrust, Wyoming, from COCORP deep-reflection data and from gravity data, *Geology*, *6*, 648–652, doi:10.1130/0091-7613(1978)6<648:NOTWRT>2.0.CO;2.

Triep, E. (1984), Mecanismos de sismos en las Sierras Pampeanas occidentales, in *Geología y Recursos Naturales de la Provincia de Río Negro: Relatorio del IX Congreso Geológico Argentino, 5 al 9 de Noviembre de 1984, San Carlos Bariloche*, pp. 61–80, Serv. Geol. Nac., Buenos Aires.

Vergés, J., V. A. Ramos, A. Meigs, E. Cristallini, F. H. Bettini, and J. M. Cortés (2007), Crustal wedging triggering recent deformation in the Andean thrust front between 31°S and 33°S: Sierras Pampeanas-Precordillera interaction, *J. Geophys. Res.*, *112*, B03S15, doi:10.1029/2006JB004287.

Wells, D. L., and K. J. Coppersmith (1994), New empirical relationships among magnitude, rupture length, rupture width, rupture area, and surface displacement, *Bull. Seismol. Soc. Am.*, *84*, 974–1002.

Wiltschko, D. V., and J. A. Dorr (1983), Timing of deformation in overthrust belt and foreland of Idaho, Wyoming, and Utah, *Am. Assoc. Pet. Geol. Bull.*, *67*, 1304–1322.

Zapata, T. R., and R. W. Allmendinger (1996), Thrust-front zone of the Precordillera, Argentina: A thick-skinned triangle zone, *Am. Assoc. Pet. Geol. Bull.*, *80*, 359–381.

A. J. Meigs, Department of Geosciences, Oregon State University, 246 Wilkinson Hall, Corvallis, OR 97331, USA. (meigsa@geo.oregonstate.edu)

J. Nabelek, College of Oceanic and Atmospheric Sciences, Oregon State University, 104 COAS Admin. Bldg., Corvallis, OR 97331, USA.